

SPP0: Efficient Long-sequence LLM Training via Adaptive Sequence Pipeline Parallel Offloading

Qiaoling Chen^{1,2,3}, Shenggui Li², Wei Gao³, Peng Sun^{3,4}, Yonggang Wen², Tianwei Zhang²
¹S-Lab, NTU ²Nanyang Technological University ³Shanghai AI Laboratory ⁴SenseTime

Abstract

In recent years, Large Language Models (LLMs) have exhibited remarkable capabilities, driving advancements in real-world applications. However, training LLMs on increasingly long input sequences imposes significant challenges due to high GPU memory and computational demands. Existing solutions face two key limitations: (1) memory reduction techniques, such as activation recomputation and CPU offloading, compromise training efficiency; (2) distributed parallelism strategies require excessive GPU resources, limiting the scalability of input sequence length.

To address these gaps, we propose Adaptive Sequence Pipeline Parallel Offloading (SPP0), a novel LLM training framework that optimizes memory and computational resource efficiency for long-sequence training. SPP0 introduces adaptive offloading, leveraging sequence-aware offloading, and two-level activation management to reduce GPU memory consumption without degrading the training efficiency. Additionally, SPP0 develops an adaptive pipeline scheduling approach with a heuristic solver and multiplexed sequence partitioning to improve computational resource efficiency. Experimental results demonstrate that SPP0 achieves up to 3.38× throughput improvement over Megatron-LM and DeepSpeed, realizing efficient training of a 7B LLM with sequence lengths of up to 4M tokens on only 128 A100 GPUs.

1 Introduction

Large Language Models (LLMs) have demonstrated exceptional capabilities, revolutionizing a multitude of domains including coding [16, 51], image processing [41, 42], video stream analysis [52, 65], and scientific research [2, 3]. As illustrated in Figure 1, the growing length of contextual information in these applications necessitates the training of LLMs to support increasingly longer sequences, from 4K tokens [55, 57] to 32K [22, 38], 128K [1, 13], and even millions of tokens [4, 9, 36, 46]. Training LLMs with such long sequence lengths imposes significant demands on GPU memory and computational resources, as the activation computation and memory in training scales with the sequence length. For example, training a GPT model with the size of 7 billion and a sequence length of 4 million tokens demands approximately 16,384GB of activation memory and necessitates at least 128 NVIDIA H100 GPUs for 105 hours to process 1 billion tokens.

Therefore, many system optimizations have been proposed to improve the memory or computational resource efficiency of long-sequence LLM training. However, they are

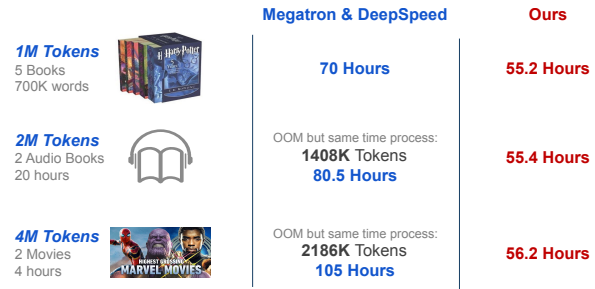


Figure 1. Performance comparisons of SPP0 and SOTA training systems on extremely long sequences of total 1B tokens, using 32, 64, and 128 GPUs, respectively.

not sufficient to achieve satisfactory performance due to the following two significant gaps.

- G1: Memory reduction techniques compromise the training efficiency.** Two prominent memory reduction techniques have been widely adopted to alleviate memory overhead in LLM training: activation recomputation [6] and CPU offloading [43]. Activation recomputation reduces the memory footprint by recomputing the activations of certain layers during backward propagation instead of storing them. Despite the significant memory savings, the recomputing step can account for up to one-third of the gradient computation time. This overhead is particularly pronounced in long-sequence training, substantially prolonging the overall training time. CPU offloading relieves GPU memory pressure by transferring activations between GPU and CPU memory. Prior offloading techniques [11, 62] operate the entire sequence of activations and assume that the overhead of CPU offloading can be effectively hidden by overlapping it with GPU computation. However, as the sequence length increases, the overhead of CPU offloading grows linearly, causing substantial delays in GPU computation and markedly degrading training efficiency. Also, existing CPU offloading techniques keep the activations of at least one layer in GPU memory, which limits their scalability for longer sequences (discussed in Section 2.1). Consequently, offloading the entire sequence of activations represents a *coarse-grained* approach, rendering current CPU offloading methods inappropriate for long-sequence training.
- G2: Distributed parallelism techniques consume excessive GPU memory and resources.** Many distributed parallelism strategies [15, 39, 56, 60] have been proposed to expedite long-sequence LLM training. However, their effectiveness relies heavily on the availability of substantial GPU

memory and resources. For instance, training a GPT model with 65 billion parameters and a sequence length of 4 million results in an activation memory footprint of 80TB, necessitating **over 1,024 NVIDIA H100 GPUs** to store activations and model weights. Such enormous resource requirements significantly hinder the scalability of sequence lengths in long-sequence training.

To address the substantial activation memory consumption of long sequences, prior works [20, 30, 33, 36] have adopted *sequence partitioning*, where long sequences are divided into multiple subsequences for processing. Building on them, we propose to *perform CPU offloading and pipeline scheduling over the subsequences, instead of the entire sequences*. We expect such adaptations could bring two potential advantages for long-sequence LLM training: (1) Subsequence-level activation offloading benefits the overlapping of GPU computation and CPU offloading. (2) Subsequence pipeline scheduling can reduce pipeline bubbles and improve training efficiency. To our best knowledge, CPU offloading and pipeline scheduling at the subsequence granularity has not been systematically studied before. However, applying them in practice still faces challenges due to their adoption of fixed offloading policy and pipeline schedule.

- **Inefficient fixed offloading.** Existing solutions commonly adopt fixed offloading policies. The length-based offloading policy [25, 61] overlooks the computational imbalance caused by later tokens requiring more computation in the attention layers. Meanwhile, the FLOPs-based offloading policy [33] achieves computational balance but at the cost of imbalanced activation memory consumption across subsequences, causing the CPU offloading overhead to outweigh GPU computation. Furthermore, fixed subsequence offloading introduces additional tensor dependencies among subsequences, resulting in unnecessary offloading overhead.
- **Inefficient fixed pipeline schedule.** The fixed pipeline schedule policy [12, 19, 39, 45] enforces a predetermined schedule for each subsequence, disregarding variations in memory and computational demands. More subsequences could increase kernel overhead and decrease throughput, while fewer subsequences could introduce high pipeline bubbles. Even with an optimized subsequence count N , pipeline bubbles remain inevitable. For example, with $p = 4$ and $N = 16$, the bubble ratio reaches $3/16$, highlighting inefficiencies in fixed schedules, where the total computation time includes both bubble overhead and execution time.

In this paper, we propose Adaptive Sequence Pipeline Parallel Offloading (SPPO), a novel framework for long-sequence LLM training. It can fully exploit the potential benefits of sequence partitioning while overcoming the limitations of existing offloading policies and pipeline schedules. SPPO partitions long input sequences into multiple subsequences and innovatively customizes *offloading* and *pipeline scheduling*

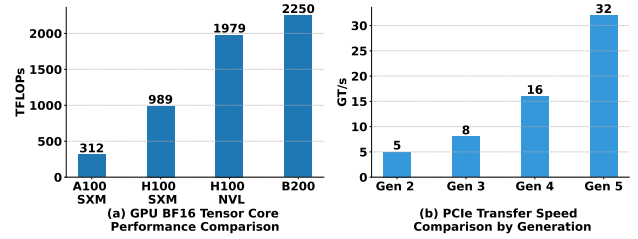


Figure 2. The evolution of GPU computing power and PCIe.

to optimize their memory and computational resource efficiency. First, SPPO designs an adaptive offloading approach to efficiently overlap the offloading of the activation of a subsequence with its computation. It consists of two key components. The first is the *sequence-aware offloading* policy to mitigate imbalanced memory allocation across subsequences. This policy adaptively computes the offload ratio to maximize the overlap between the CPU offloading for the $(i - 1)^{\text{th}}$ subsequence and the computation of the i^{th} subsequence. The second is the *two-level activation management* strategy that retains skeletal activations (i.e., those with high access frequency) in GPU memory, thereby preserving CPU-GPU bandwidth for activations with lower access frequency.

Second, we design an adaptive pipeline schedule to pipeline the computation of one subsequence in a given layer with the computation of the previous subsequence in the subsequent layer. To strike an optimal balance between GPU utilization and pipeline efficiency, we develop a *heuristic solver* to determine the ideal number of subsequences. Combined with the offloading ratio in adaptive offloading, this enables us to further improve both memory efficiency and training efficiency for long-sequence LLM training. Nevertheless, the *heuristic solver* is not always capable of eliminating resource bubbles in certain scenarios. To handle it, we introduce a *multiplexing sequence partitioning* to deliver a fine-grained partition of adjacent subsequences, further reducing the resource bubbles without sacrificing memory efficiency.

Our contributions are summarized as follows:

- We propose and implement the SPPO framework to partition long sequences into multiple subsequences. By tailoring dedicated offloading techniques and optimizing the pipeline schedule, SPPO significantly improves both memory and computational efficiency for long-sequence LLM training.
- We introduce an adaptive offloading approach, which comprises of sequence-aware offloading and two-level activation management, to maximize the overlap between CPU offloading and GPU computation.
- We design an adaptive pipeline schedule that incorporates a heuristic solver and multiplexed sequence partitioning, enhancing training efficiency without compromising the benefits from adaptive offloading.

- We evaluate SPPo through extensive experiments, demonstrating up to a 3.38× throughput improvement over Megatron-LM and DeepSpeed. Moreover, SPPo enables efficient training of a 7B LLM with sequence lengths of 1M, 2M, and 4M on only 32, 64, and 128 NVIDIA Ampere GPUs.

| | | | |
|-------|----------------------|----------|------------------------|
| B | batch size | PP | pipeline parallel size |
| H | hidden dimension | SP | sequence parallel size |
| S | sequence length | N | #subsequences |
| M_m | memory of model | s_i | subsequence i |
| M_a | memory of activation | α | offloading ratio |
| BW | bandwidth | h | hidden state |

Table 1. Notations used in this paper.

2 Background

Despite the substantial memory optimizations in attention layers achieved by FlashAttention [44, 58] and linear attention [8, 14], the linear scaling of activation memory during long-sequence LLM training still results in prohibitively high GPU memory usage. To address such overhead while maintaining computational efficiency, two primary techniques have emerged: memory reduction and distributed parallelism. However, they struggle to maintain a balance between memory efficiency and computational resource efficiency simultaneously. Table 1 illustrates the notations used in this paper.

2.1 Memory Reduction Techniques

Limited GPU memory is a critical bottleneck of training LLMs with long-sequences. To address this, the LLM community has adopted activation recomputation and offloading to reduce GPU memory consumption caused by activations. **Activation recomputation** [7, 24, 25], also referred to as activation checkpointing, reduces GPU memory usage by selectively discarding the activations of certain layers instead of retaining all intermediate activations. During backpropagation, the missing activations are recomputed on the fly. While activation recomputation alleviates the GPU memory consumption, the recomputation process brings additional computational overhead, degrading the overall training efficiency. For example, when we employ activation recomputation for all layers during long-sequence training, the cost of recomputing activations in backpropagation adds an extra 1/3 to the total computational time.

CPU Offloading [11, 50, 62] relieves the GPU memory burden by transferring activations from GPU memory to CPU and loading back to the GPU memory on demand. Unlike activation recomputation, the offloading process does not involve GPU computation. Existing offloading techniques [11, 49, 62] emphasize the ineligible cost of transferring activations between the GPU and CPU, and they attempt to maximize the overlap between the transferring process and GPU computation. However, these methods typically focus on offloading the activations of the entire input sequence for one or more layers to the CPU. During long-sequence training, the GPU

memory consumption of activations grows linearly with the sequence length, quickly saturating the CPU-GPU bandwidth. As a result, the offloading process fails to effectively overlap with GPU computation, leading to training inefficiency. Worse still, these offloading techniques need to retain the activations of the entire input sequence for at least one layer in GPU memory, which significantly limits the scalability of the sequence length. For example, when training a GPT-7B LLM with a GPU equipped with 80 GB memory, retaining activations for just one layer results in a maximum sequence length of only 128K tokens.

2.2 Distributed Parallelism Techniques

Distributed parallelism is widely adopted to expedite LLM training. It includes several key techniques, including data parallelism, tensor parallelism, pipeline parallelism, and sequence parallelism. Hybrid parallelism strategically combines multiple techniques to further accelerate training.

Data Parallelism (DP) [5, 32] segments the input data into smaller shards and distributes these shards across multiple GPUs along the batch dimension. Each GPU independently performs gradient computation, followed by gradient synchronization across GPUs with an all-reduce operation.

Tensor Parallelism (TP) [40] involves splitting model parameters of certain layers along certain dimensions across GPUs to parallelize the training process. In Megatron-LM [40], TP is employed to split linear layers by row or column dimensions, effectively reducing the GPU memory footprint of model weights while enhancing training efficiency.

Sequence Parallelism (SP) [15, 20, 25, 30, 36] divides the sequence along the sequence dimension and distributes subsequences across GPUs for parallel computation. Megatron-SP [25] leverages all-gather and reduce-scatter collectives to amortize the attention computations among GPUs and aggregate the computation results, thereby increasing the attention computation speed of long-sequence training.

Pipeline Parallelism (PP) [19, 39] partitions an LLM into several stages, distributing these pipeline stages across GPUs. During training, consecutive stages need to exchange gradients and activations. However, this dependency can result in significant GPU idle time, where computation waits for communication to complete, a phenomenon known as *pipeline bubbles*. Early works like GPipe [19] reduce pipeline bubbles via increasing the number of concurrent microbatches, albeit at the expense of higher peak memory usage. Subsequent works, including 1F1B [39] and TeraPipe [33], realize bubble reduction through careful scheduling policies.

These techniques can accelerate LLM training but require excessive GPU resources. As shown in Table 2, training sequences with lengths of 4 million tokens can require hundreds or even thousands of GPUs. Such high GPU demand primarily arises from the massive memory required for activations. For instance, training a GPT-65B model with an input

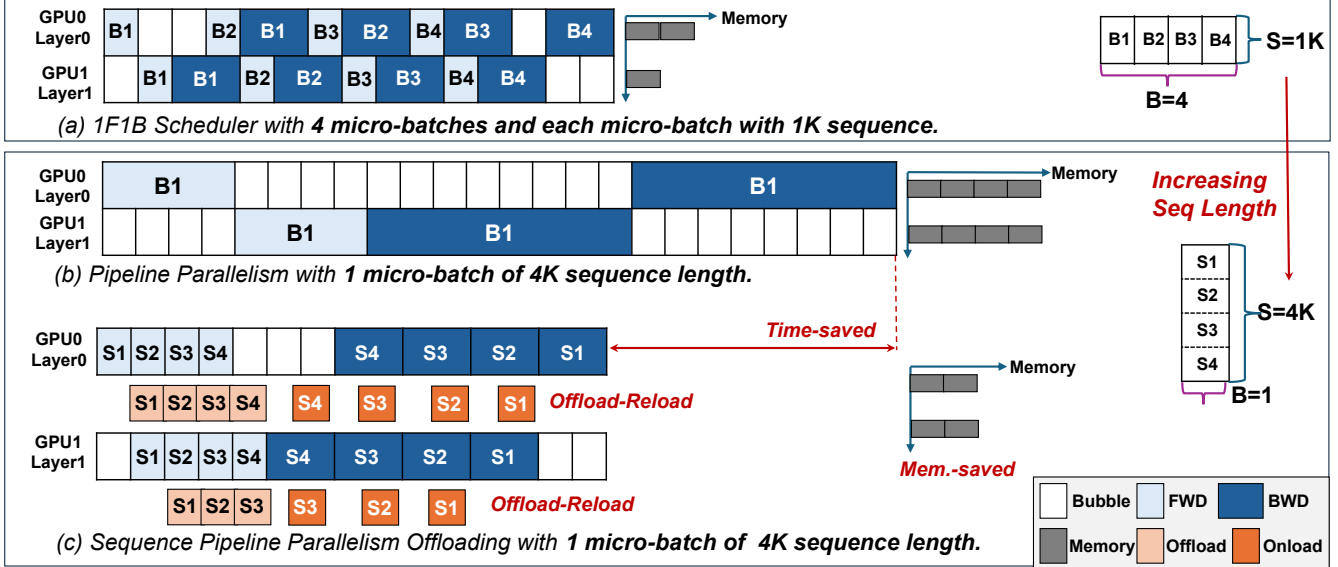


Figure 3. Illustration of the pipeline parallelism scheduling with the increasing sequence length and our sequence pipeline parallel offloading scheduling.

| Model | L | h | a | M_m | M_a | #GPUs |
|---------|----|------|----|-------|-------|-------|
| GPT-7B | 32 | 4096 | 32 | 120 | 16384 | 512+ |
| GPT-13B | 40 | 5120 | 40 | 234 | 52600 | 660+ |
| GPT-65B | 80 | 8192 | 64 | 1200 | 81920 | 1024+ |

Table 2. Training LLMs of varied sizes with sequence length of 4M tokens: memory footprint of model and activation in GB, and minimal number of A100 (80GB) GPUs required.

sequence length of one million tokens under sequence parallelism consumes 28.8 TB of activation memory, requiring at least 288 A100 GPUs to accommodate it. This underscores the critical need for an efficient approach to reduce memory consumption while maintaining training efficiency.

3 Motivation and Challenges

We first demonstrate that subsequence offloading and pipeline scheduling can provide potential memory and computational advantages over processing the entire sequence in long-sequence LLM training. Next, we investigate the impact of current subsequence offloading and pipeline schedule policies on the training efficiency. Unfortunately, neither of them can unlock the benefits offered by subsequence partitioning.

3.1 Potential Benefits

A promising approach to optimizing long-sequence LLM training is to split a long sequence into many subsequences [20, 30, 33, 36]. Thus, we can opportunistically employ CPU offloading and pipeline scheduling over *subsequences* to unleash the potential memory and computation advantages.

• **Benefit 1: Subsequence offloading.** Subsequence partition can optimize the overlapping of GPU computation and CPU offloading in two aspects. First, by partitioning the sequence into subsequences, the costs of CPU offloading

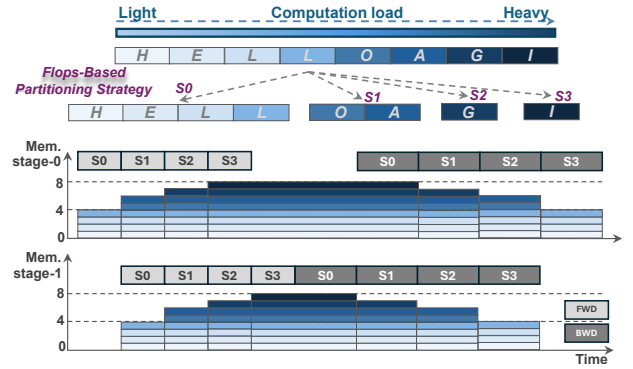


Figure 4. Background & motivation. Imbalanced computation across subsequences with its FLOPs-based offloading policy and the following memory allocation in one step.

and GPU computation become dependent on the length of the subsequences rather than the entire sequence.

Second, the CPU offloading overhead can be further reduced with the growing CPU-GPU bandwidth. As shown in Figure 2, the growth rate of CPU-GPU bandwidth has outpaced computational gains by a factor of over 30. This significant improvement in bandwidth makes it promising to hide the overhead of offloading subsequence activations to the CPU without compromising training efficiency.

• **Benefit 2: Subsequence pipeline schedule.** Incorporating subsequence partitioning with pipeline parallelism can reduce pipeline bubbles and improve training efficiency. We use a 1F1B pipeline scheduler [39] to demonstrate this in Figure 3. The 1F1B scheduler decomposes input batches into multiple micro-batches and alternates forward/backward passes as illustrated in Figure 3 (a). However, under

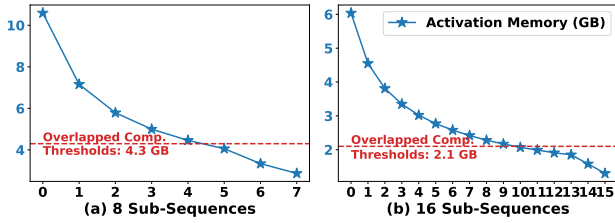


Figure 5. Activation memory allocation across subsequences when applying the optimal strategy of partitioning the sequence to 8 and 16 subsequences, respectively. The model is LLaMA-65B, and the sequence length is 128K.

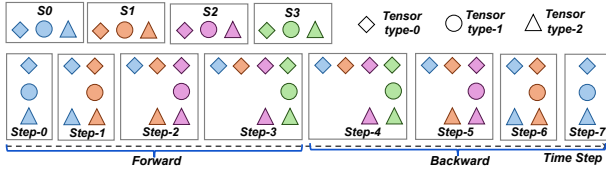


Figure 6. Transformer-based model tensor access timeline.

long-sequence inputs, the micro-batch count collapses to one, thus 1F1B degenerating to the naive pipeline schedule shown in Figure 3 (b), thereby incurring larger pipeline bubbles. As illustrated in Figure 3 (c), subsequence partitioning enables the pipelining of GPU computations for one subsequence with another. This approach reduces pipeline bubbles and maximizes resource utilization, offering a more efficient pipeline schedule for long-sequence training.

3.2 Challenge 1: Inefficient Fixed Offloading

Following previous works, a common practice is to adopt a fixed offloading policy, which can be implemented in two ways: (1) in a length-based policy [20, 25, 30, 36, 61], a consistent length is fixed across partitioned subsequences; (2) in a FLOPs-based policy [33, 54], the computational FLOPs are kept consistent among the partitioned subsequences. However, we emphasize that these fixed offloading strategies do not take into account the efficiency of the trade-offs between offloading and computation, as well as the access frequency patterns of the activation tensor, resulting in suboptimal overlapping between CPU offloading and GPU computation.

Imbalanced GPU computation across subsequences. For the attention layer, the computational load for later token positions in a sequence is heavier than that for earlier tokens [28]. However, dividing the input sequence into multiple equal-length subsequences [25, 61] overlooks this computational load imbalance. A more efficient partitioning strategy would involve starting with longer subsequences and gradually transitioning to shorter ones.

Imbalanced memory allocation across subsequences. The FLOPs-based offloading policy [33] ensures a consistent computational load across subsequences, as illustrated in Figure 4. However, due to the inherent computation imbalance in the attention layer, subsequence lengths vary under this

policy. Since the transmission overhead caused by offloading correlates linearly with the subsequence length, the FLOPs-based offloading policy cannot overlap well between the CPU offloading and GPU computation, leading to increased GPU idle time and reduced training efficiency. As shown in Figure 5, while the computational cost remains balanced under the FLOPs-based offloading policy, the size of the activations using a fixed offloading strategy varies significantly. For 8-subsequence and 16-subsequence strategies, the activation size ranges from 10.59 GB to 2.87 GB and from 6.04 GB to 1.3 GB, respectively. Correspondingly, the transmission time ranges from 821 ms to 254 ms and from 435 ms to 90 ms, respectively. Notably, for early subsequences, the transmission time exceeds the computation time, resulting in substantial offloading overhead. This highlights the need for a more fine-grained offloading policy that adapts the sequence length to maximize the overlap between computational load and activation offloading.

Unnecessary offloading overhead. Previous works have proposed to make memory offloading decisions based on the completion time of the forward pass, either at the granularity of individual layers [10, 61, 64] or batches [62]. These approaches work because the computation graph is traversed either layer-by-layer or batch-by-batch, and the intermediate activation tensors within a layer or batch are independent of those in later layers or batches. However, if we instead schedule computation at a finer granularity, such as subsequence, the tensor dependencies between subsequences increase, making offloading more complex, and the fixed offloading strategy is inefficient. To better understand the access patterns across subsequences, we profile three types of tensors at one iteration, tracking their access timestamps during both the forward and backward passes. As shown in Figure 6, Type-0 tensors (from s_0) are accessed continuously, while Type-1 tensors appear once during the forward pass and once during the backward pass. By exploiting these regular access patterns, we can derive a more intelligent and fine-grained memory offloading strategy by targeting specific tensors for offloading. For example, offloading Type-1 tensors is more efficient than offloading Type-0 and Type-2 tensors, which would otherwise incur high swapping overhead when offloaded at the subsequence granularity.

3.3 Challenge 2: Inefficient Fixed Pipeline Schedule

The fixed pipeline schedule policy, widely adopted in existing works [12, 19, 39, 45], follows a predetermined schedule for each subsequence without taking into account the varying memory and computational demands across subsequences.

Trade-off on subsequence length. Splitting a sequence into smaller subsequences introduces a trade-off between GPU utilization and pipeline efficiency. As demonstrated in Figure 7 (a), considering a single layer with a hidden dimension of 4096 and a constant sequence length of 128K, the overall forward propagation time can be mathematically

represented as the product of the number of subsequences and the time per subsequence. As the subsequence length is reduced, the total runtime escalates due to an increase in the number of subsequences and associated kernel launch overheads. Moreover, shorter subsequences lead to reduced throughput as each pipeline stage processes only a finite amount of data, thus underutilizing GPU resources. While longer subsequences are essential for higher throughput, there exists a threshold beyond which, augmenting the subsequence length ceases to enhance overall performance. This occurs as computation operators, such as attention mechanisms and generalized matrix multiplications (GEMM), stay in a compute-bound state, thereby stabilizing the total latency. On the other hand, while longer subsequences improve throughput, they introduce more pipeline bubbles, ultimately reducing overall training efficiency, as shown in Figure 7 (b). Hence, the key is to determine an *optimal* number of subsequences N to maximize the training efficiency. **Inevitable bubble overhead.** Although it is possible to find an optimal balance between GPU utilization and pipeline bubbles, efficiency inevitably suffers from the presence of pipeline bubbles. To quantify this effect in this degradation pipeline parallelism schedule, we define p as the number of pipeline stages and $F(N)$ as the time to execute the forward and backward passes for all N subsequences in a sequence. The time for a single subsequence is thus $F(N)/N$. The total pipeline bubble time t_b and bubble ratio R_b are computed as:

$$t_b = (p - 1) \cdot \frac{F(N)}{N}, R_b = \frac{p - 1}{N}.$$

Thus, the total computation time is:

$$T = t_b + F(N) = \frac{(p - 1 + N)}{N} \cdot F(N).$$

To minimize the overall computation time T , we can determine an optimal value for N . However, the pipeline bubble is inevitable by the fixed N . For example, when $p = 4$ and $N = 16$, the bubble ratio reaches a maximum of $3/16$.

4 System Overview

To enhance the memory and computational performance for long-sequence training, we propose Sequence Pipeline Parallel Offload (SPPO), a novel LLM framework that introduces innovative sequence partitioning, offloading, and pipeline scheduling customization. As mentioned in Sections 3.2 and 3.3, existing offloading and pipeline solutions exhibit several challenges in processing subsequences. Therefore, in SPPO, we introduce two approaches to address them, respectively.

- **Adaptive Offloading.** The top part of Figure 8 shows the inefficient fixed offloading (Challenge 1), which has two pipeline stages and four subsequences and employs a full offloading strategy. The offloading time of s_0 is too long, resulting in incomplete overlap with the computation. This not only delays the unloading of s_1 and increases memory

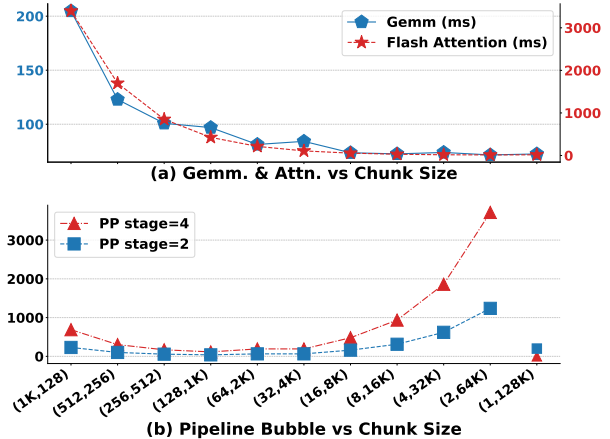


Figure 7. The relationship between subsequence length and overall forward propagation and bubble time for one transformer layer with a hidden dimension of 4096 and a fixed sequence length of 128K. The x-axis (N, s) represents a sequence of 128K length that is partitioned into N parts, and each part has s tokens.

consumption, but also delays the backward pass of s_0 , ultimately lengthening the end-to-end latency. To address Challenge 1, we introduce an **adaptive offloading** approach that effectively overlaps the offloading of activations with computation (Section 5). It refines the offloading ratio by *sequence-aware offloading* and optimizes the selection of offloaded activation by a *two-level activation management* strategy, as depicted in the middle part of Figure 8. Each subsequence tensor is divided into multiple tensor units, categorized based on their runtime lifespan and designated for either offloading or retention. At the intra-unit level, we implement two-level activation management to handle activations of varying lifespans. At the inter-unit level, we apply sequence-aware offloading, selectively deciding whether to offload tensors to CPU or retain them in GPU memory. Adaptive offloading optimizes training efficiency and reduces peak memory consumption from 7 to 5 units.

- **Adaptive Pipeline.** Despite improvements, pipeline bubbles remain an issue, as shown in Challenge 2 in the middle part of Figure 8. To further enhance pipeline efficiency, we introduce an **adaptive pipeline** mechanism. It applies a *heuristic solver* to determine the ideal number of subsequences N . To reduce pipeline bubbles, this adaptive pipeline incorporates *multiplexing sequence partitioning*, which refines subsequence partitioning to minimize resource waste without increasing memory overhead, as illustrated in the bottom part of Figure 8. By leveraging traditional sequence parallelism [20], we further partition the subsequence around pipeline bubbles into smaller sub-subsequences, distributing them across GPUs for parallel computation. For instance, s_0 in stage 0 is split into two parts, allowing forward and backward passes to execute in parallel at the beginning and

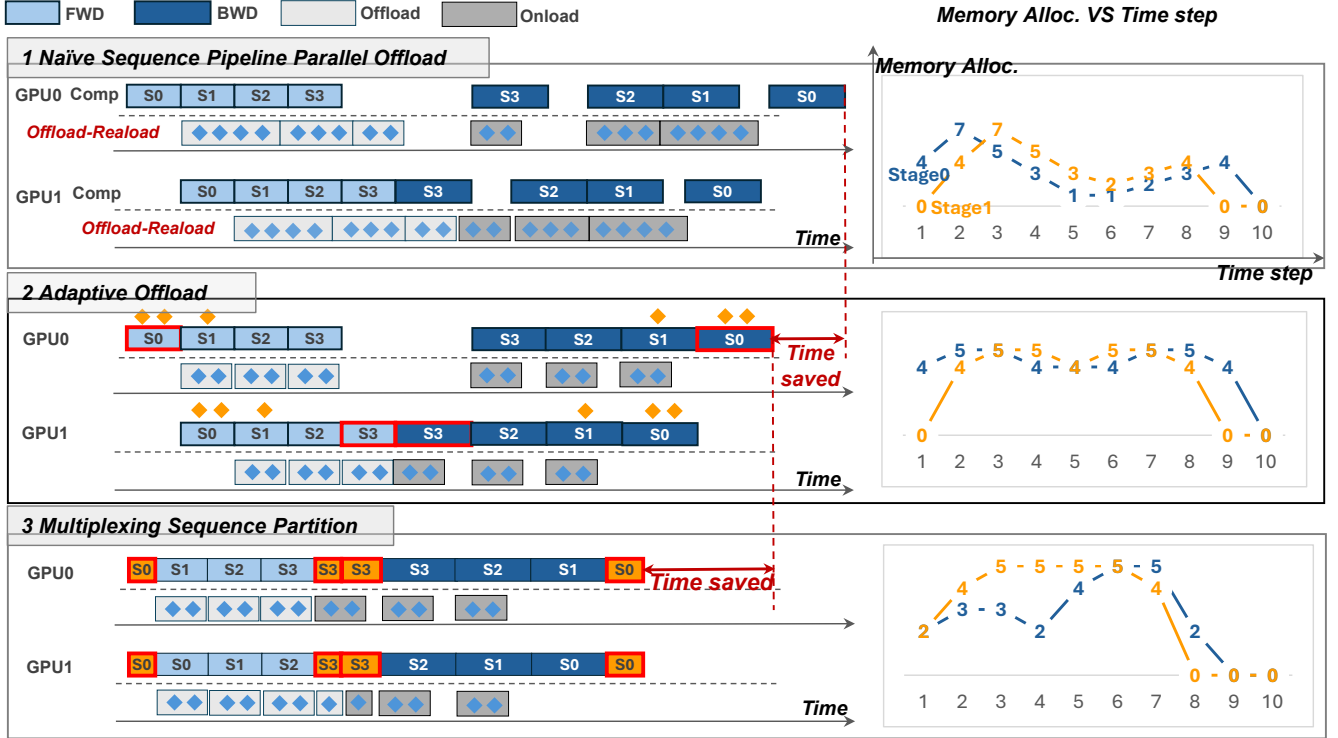


Figure 8. System Overview. The top part illustrates a minimal case of SPP0, where all subsequence activations are fully offloaded to host memory. The middle part demonstrates an adaptive offloading strategy that optimizes the minimal case, incorporating sequence-aware offloading and a two-level activation management scheme. The bottom further enhances efficiency through multiplexed sequence partitioning, achieving an almost bubble-free pipeline. The right plot visualizes the GPU activation memory allocation over time steps.

end of runtime, thereby reducing bubble time in stage 1. Similarly, s_3 in stage 1 is partitioned and computed in parallel, reducing bubble time in stage 0. SPP0 automatically recognizes those subsequences near the bubble and re-segment them without incurring additional memory overhead.

Workflow. Given a specific sequence length and available hardware resources, SPP0 operates the adaptive offloading and adaptive pipeline as follows. (1) It applies the FLOPs-based partitioning policy for balanced computation across pipeline stages instead of the length-based partition policy. Specifically, the adaptive pipeline adopts the *heuristic solver* to determine the optimal values for N and PP . (2) The adaptive offloading approach then leverages *sequence-aware offloading* to compute the offloading ratio for each subsequence and manages corresponding activations via *two-level activation management*. (3) If the pipeline scheduling still exhibits excessive bubble ratios, the adaptive pipeline applies *multiplexing sequence partitioning* to utilize these bubbles effectively, thereby enhancing training efficiency.

5 Adaptive Offloading

Traditional frameworks typically employ the same offloading strategy across layers or micro-batches. However, there exists an inherent imbalanced memory usage among different

subsequences, which leads to imbalanced transmission time across GPUs and CPU that introduces extra transmission overhead. Besides, inside subsequences, different tensors may have different lifespans. SPP0 allows each subsequence to find its best offloading strategy according to its following subsequence computation.

To search for the best offloading strategy for different subsequences, we first analyze the inner structure of the transformer layer and split the layer activation into finer-grained activation units, each of which is a minimal group of tensors to be offloaded or saved in GPUs. Then, we construct the cost model and design the algorithms to find the best offloading ratio across different subsequences.

Below, we first introduce a **two-level activation management** scheme for inner tensors within a subsequence, and then present a **sequence-aware offloading** strategy.

5.1 Two-Level Activation Management

Figure 9 (a) gives an example of how to perform the computation of subsequence s_N in a Transformer-based model, showing all skeletal tensors generated within a layer’s forward pass of s_N and their sizes. Note that, for generative LLMs, due to the casual mask, after attention computation, Q_i will not be used in the forward pass anymore, while K_i

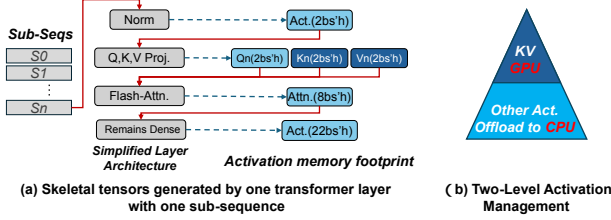


Figure 9. An example of computation of s_N in a Transformer-based model and the skeletal tensors with its sizes.

and V_i need to participate in the following Q_N computation, where $i < N$. K_0 and V_0 are Type-0 tensors that are accessed continuously (Figure 6). Therefore, we cache K_i and V_i to GPU memory instead of offloading them to CPU. Caching all $(K-V)$ pairs only consumes $\sum_{i=0}^n 2Bs_iH = 2BSH$ bytes of GPU memory, while we will partially offload the remaining $36BSH$ bytes of tensors to CPU. The offloading ratio is determined by our sequence-aware offloading strategy in Section 5.2. The most important characteristic of the remaining activations is that they are needed by backward computation, so they just need to reside in GPU memory at least before the backward propagation of the subsequence begins. Figure 9 (b) shows the architecture of our activation management.

5.2 Sequence-aware Offloading

This scheduling enables overlapping data transfer operations for the $(i-1)^{th}$ subsequence with the computation of the i^{th} subsequence, thereby reducing end-to-end training time. However, incomplete offloading of the $(i-1)^{th}$ subsequence before the completion of the i^{th} subsequence computation creates dual memory demands: the GPU must simultaneously store activation A_i and maintain an offloading buffer for A_{i-1} . As demonstrated in Figure 8 (top), this memory pressure peaks at 7 activation units when S_0 offloading persists through S_2 computation.

To address the imbalanced memory utilization, we introduce an adaptive offloading ratio $\alpha \in [0, 1]$ that controls the proportion of activations transferred to host memory. Given a FLOPs-optimized subsequence partition $s = \{s_0, s_1, \dots, s_N\}$ with $s_0 \leq s_1 \leq \dots \leq s_N$, we assign corresponding offloading ratios $\alpha = \{\alpha_0, \alpha_1, \dots, \alpha_N\}$ where $\alpha_0 \geq \alpha_1 \geq \dots \geq \alpha_N$. The memory dynamics during pipeline stage i follows:

$$M_i = M_{i-1} + A_i - (\alpha_{i-1} \cdot A_{i-1})$$

where M_i is the current GPU memory consumption, A_i is the activation volume of subsequence i , and $\alpha_{i-1} \cdot A_{i-1}$ is the offloaded portion of previous activation

We optimize α to maintain $\alpha_i \cdot A_i = M_{\text{threshold}}$, ensuring the offloading time $M_{\text{threshold}}/BW_{D2H}$ matches the balanced computation time $T_{\text{balanced_comp}}$. This constraint yields the relationship $\alpha_{i-1} \cdot A_{i-1} = \alpha_i \cdot A_i$. Peak memory M_{max} occurs when $\alpha_k = 1$ for final subsequence k , resulting in:

$$M_{\text{max}} = M_{k-1} = (1 - \alpha_{k-1}) \cdot A_{k-1}$$

| Component | Stage 0 | Stage 1 | Stage 2 | Stage 3 |
|-----------------|-----------------|-----------------|-----------------|-----------------|
| Left Seq. IDs | {0, 1, 2} | {0, 1} | {0} | 0 |
| Steady Seq. IDs | {3, 4, 5, 6, 7} | {2, 3, 4, 5, 6} | {1, 2, 3, 4, 5} | {0, 1, 2, 3, 4} |
| Right Seq. IDs | 0 | {7} | {6, 7} | {5, 6, 7} |
| Left SP Range | {0, 1, 2, 3} | {1, 2, 3} | {2, 3} | 0 |
| Right SP Range | 0 | {0, 1} | {0, 1, 2} | {0, 1, 2, 3} |

Table 3. Illustration of multiplexed sequence partitioning for $PP = 4$ stages and $N = 8$ subsequences. SP ranges denote GPU allocations for parallel computation.

This formulation enables systematic memory optimization through our proposed scheduling algorithm.

6 Adaptive Pipeline

6.1 Heuristic Solver

Given the model, sequence length s , and the number of nodes, the objective is to search for a set of hybrid parallelism parameters (SP, PP, N) that minimize the time per iteration T . To reduce the search space for performance tuning, we leverage the following heuristics:

- **Avoid cross-node sequence parallelism:** Tensor parallelism incurs significantly larger communication overhead compared to pipeline parallelism within each device, making cross-node sequence parallelism inefficient.
- **Avoid cross-node pipeline parallelism:** The P2P communication bandwidth across nodes is typically limited, leading to performance degradation.
- **Maintain near-balanced workloads:** Empirical profiling (as shown in Figure 7) suggests that the optimal workload size per layer ranges from 2K to 16K.

Following these guidelines, we restrict N within the range of 2K to 16K per layer per device, facilitating efficient workload distribution and minimizing communication overhead.

6.2 Multiplexing Sequence Partition

To address significant pipeline bubbles caused by reduced values of N , we propose a latency optimization strategy termed *multiplexing sequence partitioning*. Building on SPP0’s adaptive offloading, our method introduces finer-grained partitioning of bubble-adjacent subsequences across distributed GPUs using the traditional Megatron sequence parallelism (Section 2.2). This approach effectively minimizes idle time in pipeline stages while avoiding additional memory overhead.

Formally, for a PP -stage pipeline processing N subsequences, the forward pass of each stage consists of three computation phases:

- **Left-SP:** Initial parallel computation phase leveraging distributed subsequences.
- **Steady:** Central computation phase optimized through adaptive offloading.
- **Right-SP:** Final parallel computation phase, continuing sequence parallelism.

Each phase is characterized by three properties: (1) execution paradigm, (2) subsequence identifier mapping, and (3) communication scope. The backward pass follows a similar

yet asymmetric structure. While the Left-SP and Right-SP phases extend SPP0 with secondary sequence partitioning, the Steady phase maintains the core adaptive offloading optimization.

For pipeline stage $i \in \{0, 1, \dots, PP - 1\}$, its phase characteristics are defined as follows:

Definition 6.1 (Subsequence Identification Mapping). Given partition size $PP \in \mathbb{N}$, number of subsequences $N \in \mathbb{N}$, and stage index i , the phase-specific subsequence IDs $\mathcal{I}(i)$ are:

$$\mathcal{I}(i) = \begin{cases} \{x \in \mathbb{N}_0 \mid 0 \leq x \leq PP - 1 - i\} & \text{(Left-SP)} \\ \{x \in \mathbb{N}_0 \mid PP - 1 - i \leq x \leq N - i\} & \text{(Steady)} \\ \{x \in \mathbb{N}_0 \mid N - i \leq x \leq N - 1\} & \text{(Right-SP)} \end{cases} \quad (1)$$

where \mathbb{N}_0 denotes non-negative integers.

Definition 6.2 (Inter-Stage Communication Scope). The communication range $\mathcal{C}(i)$ for stage i is:

$$\mathcal{C}(i) = \begin{cases} \{x \in \mathbb{N}_0 \mid i \leq x \leq PP - 1\} & \text{(Left-SP)} \\ \{x \in \mathbb{N}_0 \mid 0 \leq x \leq PP - 1\} & \text{(Steady)} \\ \{x \in \mathbb{N}_0 \mid 0 \leq x \leq i\} & \text{(Right-SP)} \end{cases} \quad (2)$$

Figure 8 illustrates this mechanism: Subsequence s_0 in Stage 0 undergoes partitioning, enabling parallel execution of forward and backward passes during the initial and final phases. Simultaneously, s_3 in Stage 1 is partitioned similarly, facilitating distributed computation and reducing bubble durations in adjacent stages. Our approach dynamically identifies critical subsequences near pipeline bubbles and performs memory-efficient repartitioning without reallocation.

Table 3 illustrates this partitioning scheme for $PP = 4$ pipeline stages and $N = 8$ subsequences. The Left-SP phase processes edge subsequences near pipeline boundaries, while the Right-SP phase manages terminal computations. The Steady phase handles central subsequences using standard pipeline parallelism. Sequence parallelism ranges exhibit complementary patterns across stages, ensuring efficient resource utilization and minimizing cross-stage dependencies.

7 Evaluation

Implementation. SPP0 is implemented using Python and CUDA and encompasses around 4000 lines of code (LOC) based on Megatron-LM. The codebase consists of 2845 LOC for SPP0 optimized by adaptive offloading and 1155 LOC for multiplexing sequence partitioning. To achieve the highest bandwidth between GPU and host, we bind the Non-Uniform Memory Access node for each process and use page-locked memory for CPU buffers.

Testbed. SPP0 undergoes a thorough evaluation in the training of Transformer-based models with the GPT architecture. The size of the models range from 7 billion to 65 billion, and detailed configurations can be found in Table 2. The training process occurs on a physical cluster comprising 16 GPU servers. Each server is equipped with 8 GPUs and

128 CPU cores, a total of 128 NVIDIA Ampere GPUs. Each GPU boasts 80GB of memory. The GPUs are interconnected through NVLink and NVSwitch, while inter-node communication is facilitated by four NVIDIA Mellanox 200 Gbps HDR InfiniBand. Each node has 2 TB of CPU memory, and the GPU-CPU communication bandwidth is 32 GB/s.

Baselines and Metrics. We benchmark SPP0 against two state-of-the-art systems for long-sequence LLM training, namely DeepSpeed Ulysses [20] and Megatron-LM [25]. The evaluation metric is tokens per GPU per second (TGS) during training. By default, we enable activation checkpointing for baselines, allowing them to support longer sequence lengths. We strengthen DeepSpeed Ulysses [47] with ZeRO to reduce the memory footprint of weights, gradient, and optimizer states and with FPDT [61] to offload activations.

| Model | #GPUs | S | Mega. & SPP0 | | SPPO | Tune Mega. | | DS |
|---------|-------|-------|--------------|----|------|------------|----|----|
| | | | SP | PP | N | SP | PP | |
| GPT-7B | 32 | 512K | 8 | 4 | 32 | 32 | 1 | 32 |
| | | 640K | | | 64 | | | |
| | | 768K | | | 80 | | | |
| | | 896K | | | 128 | | | |
| | | 1024K | | | 160 | | | |
| GPT-13B | 64 | 512K | 8 | 8 | 32 | 8 | 8 | - |
| | | 640K | | | 48 | | | |
| | | 768K | | | 64 | | | |
| | | 1024K | | | 80 | | | |
| | | 1280K | | | 160 | | | |
| GPT-65B | 128 | 512K | 16 | 8 | 32 | 64 | 2 | - |
| | | 600K | | | 64 | | | |
| | | 640K | | | 80 | | | |
| | | 768K | | | 96 | | | |
| | | 1024K | | | 128 | | | |

Table 4. Configurations for various GPT models.

7.1 End-to-End Evaluation

Figure 10 illustrates the training throughput across various LLMs and sequence lengths. For fairness, we optimize the parallelism strategy for each system, as reported in Table 4. **Throughput and Scalability:** In our physical testbed, SPP0 consistently outperforms DeepSpeed-Ulysses and Megatron-LM across various sequence lengths and model sizes, achieving speedups of ranging from 1.13 \times to 3.38 \times . A key advantage of SPP0 is its ability to handle ultra-long sequences without out-of-memory (OOM) issues. In contrast, Megatron-LM struggles with sequences exceeding 896K for GPT-7B, while DeepSpeed-Ulysses fails to support sequence lengths beyond 512K for GPT-13B and GPT-65B.

Memory Efficiency: SPP0 mitigates the memory pressure through nearly zero-overhead offloading and pipeline parallelism. It avoids costly activation recomputation, a limitation that significantly impacts Megatron-LM under the same parallelism strategy. For GPT-65B, SPP0 supports sequence lengths of up to 1024K, whereas DeepSpeed-Ulysses is limited to 512K and Megatron-LM to 768K. This demonstrates SPP0’s superior memory management capabilities.

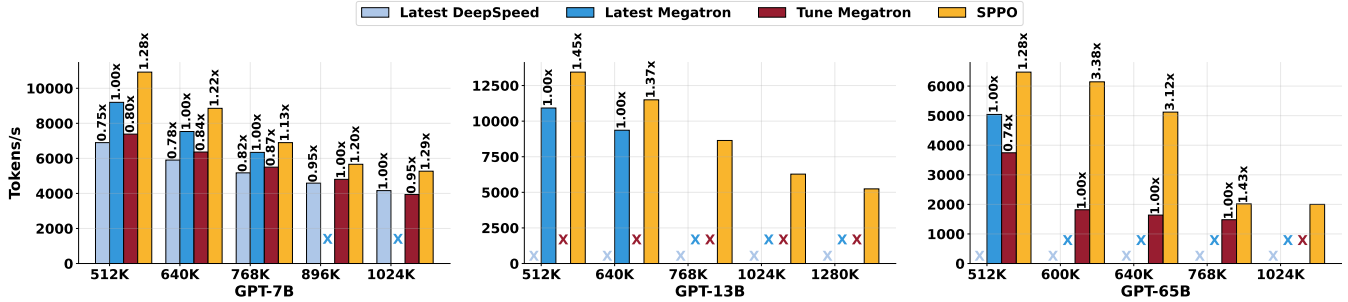


Figure 10. End-to-end evaluation results of training models of different sizes and sequence lengths.

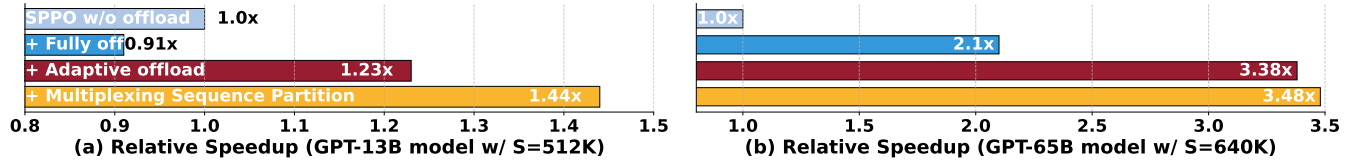


Figure 11. Breakdown analysis

Model-Specific Performance: For GPT-7B, under the same parallelism strategy as the latest Megatron-LM, SPP0 achieves a 1.13× to 1.29× speedup. At sequence lengths beyond 896K, Megatron-LM encounters OOM issues, while SPP0 continues to deliver superior throughput. For GPT-13B, SPP0 supports sequence lengths of up to 1280K, whereas Megatron-LM is limited to 768K. DeepSpeed-Ulysses cannot train GPT-13B at all due to model architectural constraints. For GPT-65B, SPP0 achieves remarkable speedups of 3.38× and 3.12× over Megatron-LM at sequence lengths of 600K and 640K, respectively. DeepSpeed-Ulysses, on the other hand, is unable to scale effectively for GPT-65B beyond 512K.

Limitations: While SPP0 shows superior performance, it is important to note that the baseline systems (DeepSpeed-Ulysses and Megatron-LM) have their own strengths in specific scenarios. For instance, Megatron-LM performs well for shorter sequence lengths (e.g., a GPT-7B model with a sequence length of 768K) despite employing activation recomputation. In such cases, SPP0 offers only marginal improvements, as the computational workload of the GPT-7B model is insufficient to fully exploit offloading overlap.

7.2 Speedup Breakdown

To gain deeper insights into the key optimizations contributing to SPP0’s benefits, we conduct a performance breakdown analysis to present the impact of each key technique. Figure 11 presents the normalized speedup performance against Megatron-LM. We have three key observations.

First, full CPU offloading alone does not always improve performance. While CPU offloading can optimize GPU memory efficiency, activation fully offloading overhead is non-negligible in certain scenarios, as discussed in Section 5 and shown in Figure 11(a). SPP0 only attains a relative speedup of 0.91 compared to SPP0 w/o offload in a GPT-13B model with

a sequence length of 512K. However, full CPU offloading benefits the parallelism strategies that exhibit high communication efficiency but poor memory efficiency, as demonstrated in Figure 11(b). It achieves a relative speedup of 2.1 × in the GPT-65B model with a sequence length of 640K.

Second, adaptive offloading consistently improves training and memory efficiency over different scenarios. Empirically, it brings a relative speedup of 1.23 × and 3.38 × for GPT-13B and GPT-65B, respectively, indicating its superiority in handling varying model sizes and sequence lengths.

Third, multiplexing sequence partitioning significantly enhances training efficiency. Its benefits are particularly pronounced when the bubble ratio is high, which is determined by the number of subsequences (N) and pipeline stages (P) used during training. MSP achieves a relative speedup of 1.44 × for the GPT-13B model and a remarkable speedup of 3.48 × for the GPT-65B model.

Overall, each optimization technique plays a pivotal role in SPP0, collectively contributing to the significant speedup demonstrated by our empirical results.

7.3 Sequence Length Scalability

To analyze the sequence length scalability of SPP0 with fixed GPU resources, we progressively increase the per-GPU sequence length from 1K to 10K tokens until experiencing OOM issues. We adopt activation checkpointing in each layer for DeepSpeed and Megatron-LM. As shown in Figure 12, SPP0 demonstrates clear advantages in sequence length scalability compared to the other two baselines.

Specifically, DeepSpeed-Ulysses partitions computation along with attention heads, making it less effective for models with a limited number of heads. For instance, the restricted number of heads in GPT-7B becomes a scalability bottleneck for DeepSpeed-Ulysses. This explains why

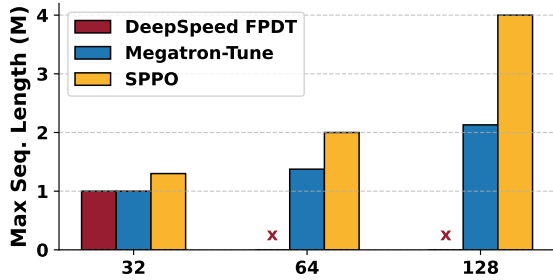


Figure 12. Scaling maximum sequence length with different number of GPUs in training GPT-7B model.

DeepSpeed-Ulysses gets a sharp decline in the maximum supported sequence length, dropping from 1K at 32 GPUs to 0 at 64 GPUs. Megatron-Tuned exhibits partial scalability (1 \times , 1.375 \times , 2.13 \times at 32/64/128 GPUs). The activation recomputation hinders the linear scaling in sequence length.

In contrast, SPPO is not constrained by the number of attention heads, achieving near-linear scalability. It can support sequence lengths of 1.3 \times , 2 \times , and 4 \times the baseline at 32, 64, and 128 GPUs, respectively. At 128 GPUs, SPPO outperforms Megatron-Tuned by 88% (4 \times vs. 2.13 \times). Moreover, SPPO achieves higher speedup at more GPUs (4 \times at 128 GPUs vs. 2 \times at 64 GPUs), indicating its ability to reduce communication overhead and enhance memory efficiency.

In sum, our empirical analysis of sequence length scalability highlights the critical role of parallelism strategies in long-sequence training. By decoupling from head-based partitioning, SPPO can flexibly adjust the configurations for parallelism strategies, enabling the training of sequences exceeding multi-million tokens. In contrast, existing LLM training systems face significant challenges in handling such extreme-scale scenarios.

8 Related Work

Systems for long-sequence training. To address memory and computational limits, ColossalAI-SP [31] introduces sequence segmentation and parallelism alongside tensor and pipeline parallelism. Ring Attention [35, 36] further improves efficiency by using blockwise self-attention to distribute long sequences across devices while overlapping key-value communication. LightSeq [27] optimizes long-sequence modeling via load balancing and re-materialization-aware checkpointing. Some approaches integrate efficient self-attention mechanisms like FlashAttention [44, 58]. Megatron-LM [25] applies sequence parallelism selectively in Dropout and LayerNorm to reduce activation redundancy, while DeepSpeed-Ulysses [20] employs all-to-all collective communication to avoid increasing overhead with sequence length. Hybrid Sequence Parallelism [15] combines Ring Attention and DeepSpeed-Ulysses to enhance scalability and efficiency.

Activation recomputation and swapping. Capuchin [43] reduces memory footprint by combining recomputation and

swapping, considering tensor access patterns. MegTaichi [17] co-optimizes tensor partitioning, while Coop [63] minimizes memory fragmentation in recomputation. These approaches do not fully leverage LLM training characteristics for optimal overlapping and fragmentation reduction. ZeRO-Offload [49] offloads optimizer states to host memory, and vDNN [50] schedules prefetching and offloading for better overlap. SuperNeurons [59] balances offloading and recomputation by offloading compute-heavy activations while recomputing lighter ones. ZeRO-Infinity [48] utilizes NVMe SSDs for large-scale training but suffers from high CPU-GPU communication costs. With modern GPUs, effectively overlapping computation with communication remains a challenge.

Reducing pipeline bubbles. Several efficient micro-batch scheduling algorithms have been proposed to mitigate the pipeline bubbles in deep learning training. GPipe [19] introduces a fill-drain schedule but suffers from pipeline inefficiencies due to warm-up and cool-down phases. PipeDream [39] employs a 1F1B schedule to reduce bubbles by executing the backward pass immediately after the forward pass of a micro-batch. DAPPLE [12] improves upon this with an early backward schedule, while Interleaved 1F1B [53] extends 1F1B with multi-stage assignments per GPU. Chimera [29, 37] implements a bidirectional pipeline with weight duplication to further reduce bubbles. Zero Bubble [45] mitigates bubbles by splitting backward computation, leveraging 1F1B scheduling and parameter gradient computation. Breadth-First [26] processes all micro-batches simultaneously in looping pipeline placement to minimize communication overhead. TeraPipe [33] and Seq1F1B [54] focus on sequence-level partitioning to balance memory and efficiency. DynaPipe [23, 34] introduces adaptive scheduling for multi-task LLM training, optimizing memory usage and communication planning. DISTMM [18] launches doubled micro-batches to circumvent dependency barriers in multi-modal training, while GraphPipe [21] preserves DNN graph topology for concurrent execution, improving pipeline efficiency and memory consumption.

9 Conclusion

In this work, we introduce Adaptive Sequence Pipeline Parallel Offloading (SPPO), a novel framework designed to enhance the efficiency of long-sequence LLM training by addressing memory and computational resource limitations. By leveraging adaptive offloading and optimized pipeline scheduling, SPPO effectively balances memory usage and training speed, overcoming the inefficiencies of existing methods. Our experimental results demonstrate significant performance improvements, achieving up to 3.38 \times higher throughput compared to state-of-the-art frameworks while reducing GPU resource requirements. These advancements pave the way for scalable and efficient training of LLMs with extremely

long input sequences, enabling broader applications across AI research and industry.

References

- [1] Josh Achiam, Steven Adler, Sandhini Agarwal, Lama Ahmad, Ilge Akkaya, Florencia Leoni Aleman, Diogo Almeida, Janko Altmenschmidt, Sam Altman, Shyamal Anadkat, et al. 2023. Gpt-4 technical report. *arXiv preprint arXiv:2303.08774* (2023).
- [2] Microsoft Research AI4Science and Microsoft Azure Quantum. 2023. The impact of large language models on scientific discovery: a preliminary study using gpt-4. *arXiv preprint arXiv:2311.07361* (2023).
- [3] Kaifeng Bi, Lingxi Xie, Hengheng Zhang, Xin Chen, Xiaotao Gu, and Qi Tian. 2023. Accurate medium-range global weather forecasting with 3D neural networks. *Nature* 619, 7970 (2023), 533–538.
- [4] Qiaoling Chen, Diandian Gu, Guoteng Wang, Xun Chen, YingTong Xiong, Ting Huang, Qinghao Hu, Xin Jin, Yonggang Wen, Tianwei Zhang, et al. 2024. Internevo: Efficient long-sequence large language model training via hybrid parallelism and redundant sharding. *arXiv preprint arXiv:2401.09149* (2024).
- [5] Qiaoling Chen, Qinghao Hu, Zhisheng Ye, Guoteng Wang, Peng Sun, Yonggang Wen, and Tianwei Zhang. 2023. AMSF: Super-Scaling LLM Training via Advanced Model States Partitioning. *CoRR abs/2311.00257* (2023).
- [6] Tianqi Chen, Bing Xu, Chiyuan Zhang, and Carlos Guestrin. 2016. Training deep nets with sublinear memory cost. *arXiv preprint arXiv:1604.06174* (2016).
- [7] Tianqi Chen, Bing Xu, Chiyuan Zhang, and Carlos Guestrin. 2016. Training deep nets with sublinear memory cost. *arXiv preprint arXiv:1604.06174* (2016).
- [8] Tri Dao and Albert Gu. 2024. Transformers are SSMs: Generalized models and efficient algorithms through structured state space duality. *arXiv preprint arXiv:2405.21060* (2024).
- [9] Kimi Developers. 2024. kimi. <https://kimi.moonshot.cn/>
- [10] NVIDIA Developers. 2023. NVIDIA Transformer Engine Offloading strategy. https://docs.nvidia.com/deeplearning/transformer-engine/user-guide/api/pytorch.html#transformer_engine.pytorch.get_cpu_offload_context
- [11] NVIDIA Developers. 2023. TransformerEngine. <https://github.com/NVIDIA/TransformerEngine>
- [12] Shiqing Fan, Yi Rong, Chen Meng, Zongyan Cao, Siyu Wang, Zhen Zheng, Chuan Wu, Guoping Long, Jun Yang, Lixue Xia, et al. 2021. DAPPLE: A pipelined data parallel approach for training large models. In *Proceedings of the 26th ACM SIGPLAN Symposium on Principles and Practice of Parallel Programming*. 431–445.
- [13] Yao Fu, Rameswar Panda, Xinyao Niu, Xiang Yue, Hannaneh Hajishirzi, Yoon Kim, and Hao Peng. 2024. Data engineering for scaling language models to 128k context. *arXiv preprint arXiv:2402.10171* (2024).
- [14] Albert Gu and Tri Dao. 2023. Mamba: Linear-time sequence modeling with selective state spaces. *arXiv preprint arXiv:2312.00752* (2023).
- [15] Diandian Gu, Peng Sun, Qinghao Hu, Ting Huang, Xun Chen, YingTong Xiong, Guoteng Wang, Qiaoling Chen, Shangchun Zhao, Jiarui Fang, et al. 2024. Loongtrain: Efficient training of long-sequence llms with head-context parallelism. *arXiv preprint arXiv:2406.18485* (2024).
- [16] Daya Guo, Qihao Zhu, Dejian Yang, Zhenda Xie, Kai Dong, Wentao Zhang, Guanting Chen, Xiao Bi, Yu Wu, YK Li, et al. 2024. DeepSeek-Coder: When the Large Language Model Meets Programming—The Rise of Code Intelligence. *arXiv preprint arXiv:2401.14196* (2024).
- [17] Zhongzhe Hu, Junmin Xiao, Zheyang Deng, Mingyi Li, Kewei Zhang, Xiaoyang Zhang, Ke Meng, Ninghui Sun, and Guangming Tan. 2022. MegTaiChi: Dynamic tensor-based memory management optimization for DNN training. In *Proceedings of the 36th ACM International Conference on Supercomputing*. 1–13.
- [18] Jun Huang, Zhen Zhang, Shuai Zheng, Feng Qin, and Yida Wang. 2024. {DISTMM}: Accelerating Distributed Multimodal Model Training. In *21st USENIX Symposium on Networked Systems Design and Implementation (NSDI 24)*. 1157–1171.
- [19] Yanping Huang, Youlong Cheng, Ankur Bapna, Orhan Firat, Mia Xu Chen, Dehao Chen, HyoukJoong Lee, Jiquan Ngiam, Quoc V. Le, Yonghui Wu, and Zhifeng Chen. 2019. GPipe: efficient training of giant neural networks using pipeline parallelism. In *Proceedings of the 33rd International Conference on Neural Information Processing Systems (NIPS’19)*. Curran Associates Inc.
- [20] Sam Ade Jacobs, Masahiro Tanaka, Chengming Zhang, Minjia Zhang, Shuaiwen Leon Song, Samyam Rajbhandari, and Yuxiong He. 2023. DeepSpeed Ulysses: System Optimizations for Enabling Training of Extreme Long Sequence Transformer Models. *CoRR abs/2309.14509* (2023).
- [21] Byungsoo Jeon, Mengdi Wu, Shiyi Cao, Sunghyun Kim, Sunghyun Park, Neeraj Aggarwal, Colin Unger, Daiyaan Arfeen, Peiyuan Liao, Xupeng Miao, et al. 2024. Graphpipe: Improving performance and scalability of dnn training with graph pipeline parallelism. *arXiv preprint arXiv:2406.17145* (2024).
- [22] Albert Q Jiang, Alexandre Sablayrolles, Arthur Mensch, Chris Bamford, Devendra Singh Chaplot, Diego de las Casas, Florian Bressand, Gianna Lengyel, Guillaume Lample, Lucile Hussenot, et al. 2023. Mistral 7B. *arXiv preprint arXiv:2310.06825* (2023).
- [23] Chenyu Jiang, Zhen Jia, Shuai Zheng, Yida Wang, and Chuan Wu. 2024. DynaPipe: Optimizing multi-task training through dynamic pipelines. In *Proceedings of the Nineteenth European Conference on Computer Systems*. 542–559.
- [24] Marisa Kirisame, Steven Lyubomirsky, Altan Haan, Jennifer Brennan, Mike He, Jared Roesch, Tianqi Chen, and Zachary Tatlock. 2020. Dynamic tensor rematerialization. *arXiv preprint arXiv:2006.09616* (2020).
- [25] Vijay Anand Korthikanti, Jared Casper, Sangkug Lym, Lawrence McAfee, Michael Andersch, Mohammad Shoeybi, and Bryan Catanzaro. 2023. Reducing activation recomputation in large transformer models. *Proceedings of Machine Learning and Systems* 5 (2023), 341–353.
- [26] Joel Lamy-Poirier. 2023. Breadth-first pipeline parallelism. *Proceedings of Machine Learning and Systems* 5 (2023), 48–67.
- [27] Dacheng Li, Rulin Shao, Anze Xie, Eric P Xing, Joseph E Gonzalez, Ion Stoica, Xuezhe Ma, and Hao Zhang. 2023. LightSeq: Sequence Level Parallelism for Distributed Training of Long Context Transformers. *arXiv preprint arXiv:2310.03294* (2023).
- [28] Dacheng Li, Rulin Shao, Anze Xie, Eric P Xing, Xuezhe Ma, Ion Stoica, Joseph E Gonzalez, and Hao Zhang. 2023. Distflashattn: Distributed memory-efficient attention for long-context llms training. *arXiv preprint arXiv:2310.03294* (2023).
- [29] Shigang Li and Torsten Hoefler. 2021. Chimera: efficiently training large-scale neural networks with bidirectional pipelines. In *Proceedings of the International Conference for High Performance Computing, Networking, Storage and Analysis (SC ’21)*. Association for Computing Machinery.
- [30] Shenggui Li, Fuzhao Xue, Chaitanya Baranwal, Yongbin Li, and Yang You. 2021. Sequence parallelism: Long sequence training from system perspective. *arXiv preprint arXiv:2105.13120* (2021).
- [31] Shenggui Li, Fuzhao Xue, Chaitanya Baranwal, Yongbin Li, and Yang You. 2022. Sequence Parallelism: Long Sequence Training from System Perspective. *CoRR abs/2105.13120* (2022).
- [32] Shen Li, Yanli Zhao, Rohan Varma, Omkar Salpekar, Pieter Noordhuis, Teng Li, Adam Paszke, Jeff Smith, Brian Vaughan, Pritam Damania, and Soumith Chintala. 2020. PyTorch Distributed: Experiences on Accelerating Data Parallel Training. *CoRR abs/2006.15704* (2020).
- [33] Zhuohan Li, Siyuan Zhuang, Shiyuan Guo, Danyang Zhuo, Hao Zhang, Dawn Song, and Ion Stoica. 2021. TeraPipe: Token-Level

- Pipeline Parallelism for Training Large-Scale Language Models. *CoRR* abs/2102.07988 (2021).
- [34] Zhiqi Lin, Youshan Miao, Guanbin Xu, Cheng Li, Olli Saarikivi, Saeed Maleki, and Fan Yang. 2024. Tessel: Boosting distributed execution of large dnn models via flexible schedule search. In *2024 IEEE International Symposium on High-Performance Computer Architecture (HPCA)*. IEEE, 803–816.
- [35] Hao Liu and Pieter Abbeel. 2023. Blockwise Parallel Transformer for Large Context Models. *CoRR* abs/2305.19370 (2023).
- [36] Hao Liu, Matei Zaharia, and Pieter Abbeel. 2023. Ring Attention with Blockwise Transformers for Near-Infinite Context. *CoRR* abs/2310.01889 (2023).
- [37] Ziming Liu, Shenggan Cheng, Haotian Zhou, and Yang You. 2023. Hanayo: Harnessing Wave-like Pipeline Parallelism for Enhanced Large Model Training Efficiency. *CoRR* abs/2308.15762 (2023).
- [38] LLaMA2-7B-32K. 2022. LLaMA2-7B-32K. <https://huggingface.co/togethercomputer/LLaMA-2-7B-32K>
- [39] Deepak Narayanan, Aaron Harlap, Amar Phanishayee, Vivek Seshadri, Nikhil R. Devanur, Gregory R. Ganger, Phillip B. Gibbons, and Matei Zaharia. 2019. PipeDream: generalized pipeline parallelism for DNN training. In *Proceedings of the 27th ACM Symposium on Operating Systems Principles (SOSP '19)*. Association for Computing Machinery.
- [40] Deepak Narayanan, Mohammad Shoeybi, Jared Casper, Patrick LeGresley, Mostofa Patwary, Vijay Anand Korthikanti, Dmitri Vainbrand, Prithvi Kashinkunti, Julie Bernauer, Bryan Catanzaro, Amar Phanishayee, and Matei Zaharia. 2021. Efficient Large-Scale Language Model Training on GPU Clusters Using Megatron-LM. *CoRR* abs/2104.04473 (2021).
- [41] Houlby Neil and Weissenborn Dirk. 2020. Transformers for Image Recognition at Scale. *Online: <https://ai.googleblog.com/2020/12/transformers-for-image-recognition-at-scale.html>* (2020).
- [42] William Peebles and Saining Xie. 2023. Scalable diffusion models with transformers. In *Proceedings of the IEEE/CVF International Conference on Computer Vision*. 4195–4205.
- [43] Xuan Peng, Xuanhua Shi, Hulin Dai, Hai Jin, Weiliang Ma, Qian Xiong, Fan Yang, and Xuehai Qian. 2020. Capuchin: Tensor-based gpu memory management for deep learning. In *Proceedings of the Twenty-Fifth International Conference on Architectural Support for Programming Languages and Operating Systems*. 891–905.
- [44] PyTorch. 2023. Accelerating Large Language Models with Accelerated Transformers. <https://pytorch.org/blog/accelerating-large-language-models/>.
- [45] Penghui Qi, Xinyi Wan, Guangxing Huang, and Min Lin. 2023. Zero bubble pipeline parallelism. *arXiv preprint arXiv:2401.10241* (2023).
- [46] qwen Developers. 2024. qwen. <https://tongyi.aliyun.com/qianwen/>
- [47] Samyam Rajbhandari, Jeff Rasley, Olatunji Ruwase, and Yuxiong He. 2020. ZeRO: memory optimizations toward training trillion parameter models. In *Proceedings of the International Conference for High Performance Computing, Networking, Storage and Analysis (SC '20)*. IEEE Press.
- [48] Samyam Rajbhandari, Olatunji Ruwase, Jeff Rasley, Shaden Smith, and Yuxiong He. 2021. ZeRO-Infinity: Breaking the GPU Memory Wall for Extreme Scale Deep Learning. *CoRR* abs/2104.07857 (2021).
- [49] Jie Ren, Samyam Rajbhandari, Reza Yazdani Aminabadi, Olatunji Ruwase, Shuangyan Yang, Minjia Zhang, Dong Li, and Yuxiong He. 2021. {Zero-offload}: Democratizing {billion-scale} model training. In *2021 USENIX Annual Technical Conference (USENIX ATC 21)*. 551–564.
- [50] Minsoo Rhu, Natalia Gimelshein, Jason Clemons, Arslan Zulfiqar, and Stephen W Keckler. 2016. vDNN: Virtualized deep neural networks for scalable, memory-efficient neural network design. In *2016 49th Annual IEEE/ACM International Symposium on Microarchitecture (MICRO)*. IEEE, 1–13.
- [51] Baptiste Roziere, Jonas Gehring, Fabian Gloeckle, Sten Sootla, Itai Gat, Xiaoqing Ellen Tan, Yossi Adi, Jingyu Liu, Romain Sauvestre, Tal Remez, et al. 2023. Code llama: Open foundation models for code. *arXiv preprint arXiv:2308.12950* (2023).
- [52] Ludan Ruan and Qin Jin. 2022. Survey: Transformer based video-language pre-training. *AI Open* 3 (2022), 1–13.
- [53] Mohammad Shoeybi, Mostofa Patwary, Raul Puri, Patrick LeGresley, Jared Casper, and Bryan Catanzaro. 2020. Megatron-LM: Training Multi-Billion Parameter Language Models Using Model Parallelism. *CoRR* abs/1909.08053 (2020).
- [54] Ao Sun, Weilin Zhao, Xu Han, Cheng Yang, Xinrong Zhang, Zhiyuan Liu, Chuan Shi, and Maosong Sun. 2024. Seq1f1b: Efficient sequence-level pipeline parallelism for large language model training. *arXiv preprint arXiv:2406.03488* (2024).
- [55] Rohan Taori, Ishaan Gulrajani, Tianyi Zhang, Yann Dubois, Xuechen Li, Carlos Guestrin, Percy Liang, and Tatsunori B Hashimoto. 2023. Alpaca: A strong, replicable instruction-following model. *Stanford Center for Research on Foundation Models. <https://crfm.stanford.edu/2023/03/13/alpaca.html>* 3, 6 (2023), 7.
- [56] Jakub M. Tarnawski, Deepak Narayanan, and Amar Phanishayee. 2021-12-06. Piper: Multidimensional Planner for DNN Parallelization. In *Advances in Neural Information Processing Systems (NeurIPS '21)*.
- [57] Hugo Touvron, Louis Martin, Kevin Stone, Peter Albert, Amjad Almahairi, Yasmine Babaei, Nikolay Bashlykov, Soumya Batra, Prajwal Bhargava, Shrutvi Bhosale, et al. 2023. Llama 2: Open foundation and fine-tuned chat models. *arXiv preprint arXiv:2307.09288* (2023).
- [58] Patrick von Platen. 2023. Optimizing your LLM in production. <https://huggingface.co/blog/optimize-llm>.
- [59] Linnan Wang, Jinmian Ye, Yiyang Zhao, Wei Wu, Ang Li, Shuaiwen Leon Song, Zenglin Xu, and Tim Kraska. 2018. Superneurons: Dynamic GPU memory management for training deep neural networks. In *Proceedings of the 23rd ACM SIGPLAN symposium on principles and practice of parallel programming*. 41–53.
- [60] Fuzhao Xue, Yukang Chen, Dacheng Li, Qinghao Hu, Ligeng Zhu, Xiuyu Li, Yunhao Fang, Haotian Tang, Shang Yang, Zhijian Liu, et al. 2024. Longvila: Scaling long-context visual language models for long videos. *arXiv preprint arXiv:2408.10188* (2024).
- [61] Jinghan Yao, Sam Ade Jacobs, Masahiro Tanaka, Olatunji Ruwase, Aamir Shafi, Hari Subramoni, and Dhableswar K Panda. 2024. Training Ultra Long Context Language Model with Fully Pipelined Distributed Transformer. *arXiv preprint arXiv:2408.16978* (2024).
- [62] Tailing Yuan, Yuliang Liu, Xucheng Ye, Shenglong Zhang, Jianchao Tan, Bin Chen, Chengru Song, and Di Zhang. 2024. Accelerating the training of large language models using efficient activation rematerialization and optimal hybrid parallelism. In *2024 USENIX Annual Technical Conference (USENIX ATC 24)*. 545–561.
- [63] Jianhao Zhang, Shihan Ma, Peihong Liu, and Jinhui Yuan. 2023. Coop: Memory is not a Commodity. *Advances in Neural Information Processing Systems* 36 (2023), 49870–49882.
- [64] Pinxue Zhao, Hailin Zhang, Fangcheng Fu, Xiaonan Nie, Qibin Liu, Fang Yang, Yuanbo Peng, Dian Jiao, Shuaipeng Li, Jinbao Xue, et al. 2024. Efficiently Training 7B LLM with 1 Million Sequence Length on 8 GPUs. *arXiv preprint arXiv:2407.12117* (2024).
- [65] Zangwei Zheng, Xiangyu Peng, Tianji Yang, Chenhui Shen, Shenggui Li, Hongxin Liu, Yukun Zhou, Tianyi Li, and Yang You. 2024. OpenSora: Democratizing efficient video production for all. *arXiv preprint arXiv:2412.20404* (2024).